PRELIMINARY AERODYNAMIC INVESTIGATION OF BOX-WING CONFIGURATIONS USING LOW FIDELITY CODES

F. A. Khan, P. Krammer, D. Scholz
Hamburg University of Applied Sciences
Aero – Aircraft Design and Systems Group
Berliner Tor 9, D-20099 Hamburg, Germany

Abstract

This paper outlines the different aerodynamic aspects of box-wing design i.e. an unconventional aircraft design configuration exhibiting the capability of reducing induced drag. To understand basic aerodynamic features and their influence on box-wing aerodynamics, parameter variations have been conducted while Munk's theorem is validated for stagger and sweep. In this process, several important aspects of box-wing are highlighted. An optimization algorithm has been implemented by considering all the design variables collectively to find the global maximum for the box-wing design. All these investigations laid down the important aerodynamic features of box-wing and also proved a method for estimating the reduction in induced drag. To conduct these investigations, vortex lattice methods (VLM) are used. Nonplanar systems have certain limitations for best operations which provide maximum induced drag reduction. These limitations are examined and applied in the form of constant and specified lift distributions in the analysis. Furthermore, it is concluded that vortex lattice methods do capture the reduction in induced drag correctly if the limitations of span loading are maintained during the analysis. Based on previous results obtained, Euler inviscid analysis for a selected box-wing and a reference wing are carried out. The results of Euler inviscid analysis show good agreement with the results achieved by vortex lattice method in drag reduction at low Mach number. At the same time, transonic airfoil selection is identified as one of the key factors in designing a commercial box-wing aircraft for the transonic flight regime. This study is closed up by discussing different potential advantages and highlighting the main aspects in box-wing design.

1. INTRODUCTION

Air traffic is predicted to grow at a rate of 5% annually, resulting in a rapid increase of carbon emissions for aviation industry. Combined with uncertainties of aviation contributions to climate change, there has never been such a tremendous need for improved and efficient civil transport aircraft [1].

As far as current conventional aircrafts are concerned, designs are optimized to achieve highest levels of performance and it would be extremely difficult to come up with new design solutions for the future out of the existing trends.

Unconventional, novel concepts like nonplanar designs exhibit reduction in drag as compared to conventional planar wings of same span and lift [2]. Drag reduction results in a direct decrease in operating costs and in an in-direct decrease in noise and emissions levels. Drag during the cruise phase of large transport aircraft consists of friction and induced drag, where the induced drag is relatively lower than the friction drag. But still, induced drag consists of 43% of the total drag budget [3]. Thus, any reduction in induced drag will directly improve the efficiency of the overall design. Moreover, induced drag is also coupled with viscous or friction drag [2], thus its reduction can be beneficial in a greater extent than actually comprehended.

This study is primarily based on finding an insight into the unique aerodynamic characteristics of box-wing configurations, with aims to outline and capture the important factors of the design for drag reduction which can consequently lead to performance improvements.

2. DRAG REDUCTION

Drag is the aerodynamic force that opposes an aircraft's motion through the air. From the early days of aviation, aerodynamicists have been trying to minimize the drag by direct and in-direct methods. Drag equals the power required from the propulsion system of the aircraft during its cruise stage (for civil transport aircraft the cruise segment comprises almost 90% of flight time). Thus it directly corresponds to the amount of power required, fuel consumed and resultantly the overall weight of the aircraft.

In coefficient form, drag can be written as:

(1) $C_D = C_{D0} + C_{Di}$ Where: $C_{Di} = C_{Di_{M\to 0}} + C_{Di_M}$

Zero lift drag (C_{D0}) or drag due to friction has an

incompressible and compressible components. Similarly to that, C_{Di} is drag due to lift and can be divided into induced drag at lower Mach number and compressibility drag due to lift at Mach number higher than 0.3.

2.1. Induced Drag

Lift is generated by the pressure differential created by the airfoil section along the span of the wing. For finite wings (3D flow) this pressure differential causes the flow at wing tips to curl around and thus forming circular flow near the wing tips, which results in generation of wingtip vortices. This vortex system in-return causes a downward component of velocity along the span called *downwash.* The downwash combined with free stream relative to wind velocity, reduces the effective angle of attack along the span. This reduction in angle of attack results in a local inclination of the lift vector relative to the incoming velocity vector and produces an *induced drag* [4].

The coefficient of induced drag component can be separately written as:

$$C_{Di} = {C_L}^2 / \pi \cdot e \cdot AR \tag{2}$$

Here, *e* is called Oswald's efficiency factor or span efficiency factor and accounts for the nonoptimal lift distribution along the span. For planar wings, if the spanwise lift distribution is elliptical, *e* attains a maximum value of unity.

It is important to note here, that induced drag increases rapidly as lift coefficient is increased. For civil transport aircrafts this happens during take-off, climb and landing flight segments. Alternatively, the parasite drag decreases with decrease in flight speed. Thus it can be seen that by a reduction in induced drag the aircraft can benefit in all segments of its mission and not only in the cruise stage. As aircraft are designed in keeping all the segments of operation in similar perspective, an induced drag reduction also occurs e.g. during take-off and it will change conditions associated with engine-out climb. Changes in aircraft performance at these conditions influence the overall design and thus have an indirect, but powerful effect on the aircraft cruise performance [5].

From Equation (2), it can be seen that an induced drag reduction can be carried out by increasing the aspect ratio and/or the span efficiency factor. Increasing the aspect ratio means increasing the span of the wing while keeping the reference area constant. With the increase in span, the vortex strength along the tips is decreased and consequently the reduction in effective angle of attack is less compared to small aspect ratio wings.

Although increasing span has aerodynamic benefits, structurally it is not the best option, as its increase results in aero elastic problems of the wing. The centre of lift moves towards the tip, resulting in the need of a stronger internal structure to compensate for the additional force. In return, to make the structure stronger, additional mass is added to the aircraft, which in itself reduces the overall performance of the design. Another problem due to increase in span is increased airport terminal restrictions. Currently the maximum space allotted for aircraft parking at terminals is an 80x80 m box. The Airbus A380 has a span of 79.8 m just below the 80 m box limit. If the wing loading for the Airbus A380 would be similar to that of an Airbus A340 it would have resulted in a span of 102 m, which as a result, would improve the performance along with a decrease in specific fuel consumption and wing area [6]. Thus it can be observed that the increase in span has its benefits but the hurdles associated with it make it a challenging task.

2.2. Nonplanar Concepts for Induced Drag Reduction

Another approach for induced drag reduction can be obtained by increasing the span efficiency factor. As mentioned before for a planar wing having a given span and lift, the maximum span efficiency factor is limited to unity. For nonplanar systems span efficiency factor can be increased beyond unity.

Several nonplanar concepts are shown in Figure 1. It shows the front views of different wing layouts. It can be seen that the box-wing configuration shown in bottom right has the maximum span efficiency out of all configurations shown.

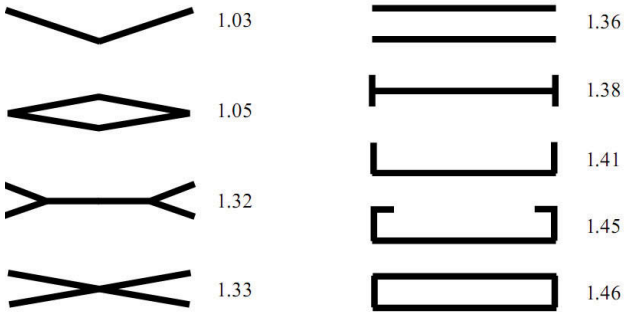

FIG 1. Span efficiencies for various optimally loaded nonplanar system (h/b=0.2) [5]

Some of the layouts take advantage of reduction in induced drag by end plates (or winglets) at wing tips. Others have an increased aspect ratio for individual wings by distributing one wing into multiple wings having same span and same total area. A box-wing configuration takes advantage from both aspects.

The results shown in Figure 1 were obtained with a height to span ratio of 0.2. If this ratio is increased, the span efficiencies can even go higher because the mutual interference drag reduces as the gap between the lifting surfaces is increased.

2.3. Box-Wing Configuration

The concept of box-wing was presented by Prandtl in 1924. According to his findings, the biplane has lesser drag than an equivalent monoplane and its minimum drag is obtained when two wings of biplane are of same span [7]. Further on, more reduction in induced drag is possible if wing end plates are attached to the wing tips thus making it a closed system.

To gain maximum benefit out of the box-wing system it must have same lift distribution (constant component added to elliptical distribution) and same total lift on each of the horizontal wings and butterfly shaped lift distribution on the vertical tip wings (Figure 2). When these conditions of minimum occur, the velocity induced by the free vortices is constant along the two horizontal wings and identically zero on the vertical side wings. The induced drag decreases for increasing non-dimensional gap [8].

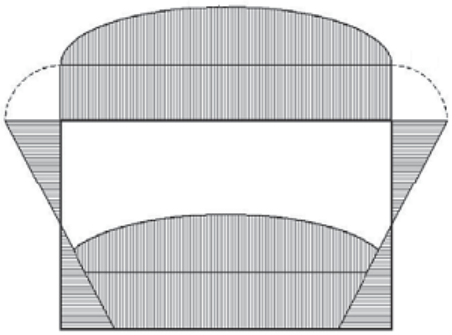

FIG 2. Box-wing spanwise lift distribution shown in front view [9]

In addition to reductions in induced drag, the box-wing configuration has desirable effects on structures, stability and control characteristics, vortex wake hazards, and other practical aspects of the design [2].

In 1921, Munk presented interesting results for nonplanar configurations that if the circulation of each element in wing systems is kept constant, then the total induced drag of the system will remain the same. In other words the induced drag is independent of the longitudinal position of the lifting surface as long as the total circulation for each surface is held constant. This is known as *Munk's stagger theorem* and is of great importance in evaluating concepts for induced drag reduction [5].

If the box-wing configuration is studied more carefully it can be seen that it is a combination of two wings having winglets attached at their tips. The lower wing has a winglet which has a 0° cant angle (right angled, upward) while the upper wing has a winglet with 180° cant angle (right angled, downward) such that both winglets are connected at their tips. This wing-winglet combination has minimum induced drag when the velocity normal to the winglet is zero. This happens when the sidewash produced on the winglet by the wing exactly cancels the sidewash produced by the winglet on itself. In other words, the induced angle of attack of the winglet is zero. The induced drag of the wing is minimized by the presence of a winglet since the winglet causes a reduction in the net downwash at the wing; hence, the induced angle of attack is reduced [10].

3. MOTIVATION

Through literature review, it can be concluded that nonplanar configurations do have the potential to lead the aviation industry in the future. At the same time, it can be seen that nonplanar configurations are different from conventional designs in-terms of aerodynamic and structural requirements needed to operate them successfully. Thus the design procedure required for constructing a successful nonplanar aircraft would be different from existing conventional aircrafts.

As far as box-wing is concerned, it is reducing drag by two techniques: firstly the presence of winglets increases the span efficiency and secondly, dividing the single wing into two wings having double or slightly less aspect ratios (depending on structural constraints) improves the induced drag according to the basic aerodynamic theory. The box-wing design seems to have the potential to prove beneficial in both aerodynamics and structural domains, thus in-depth analysis of this configuration should be carried out to truly understand the limitations of this design.

4. ANALYSIS APPROACH

The analysis approach for the following work is to first outline the basics of box-wing design and to elaborate its design drivers. The goal is to investigate possible design issues of box-wing configurations. At this preliminary stage of analysis, low fidelity aerodynamic codes are used to explore the variation of these design drivers. Further on, a higher order method is used i.e., the Euler CFD method, to carry out further investigations of box-wing design.

In the following sections, different geometrical aspects of the box-wing will be discussed in detail. Thus it is important here to highlight and point out these fundamental geometrical aspects shown in Figure 3.

Following aims of the study are to be met (by performing the above stated analysis);

- Exploring a possible way of investigating futuristic multi planar aircraft configurations
- Identifying key design variables for box-wing configuration
- Verifying Munk's theorem for sweep and stagger

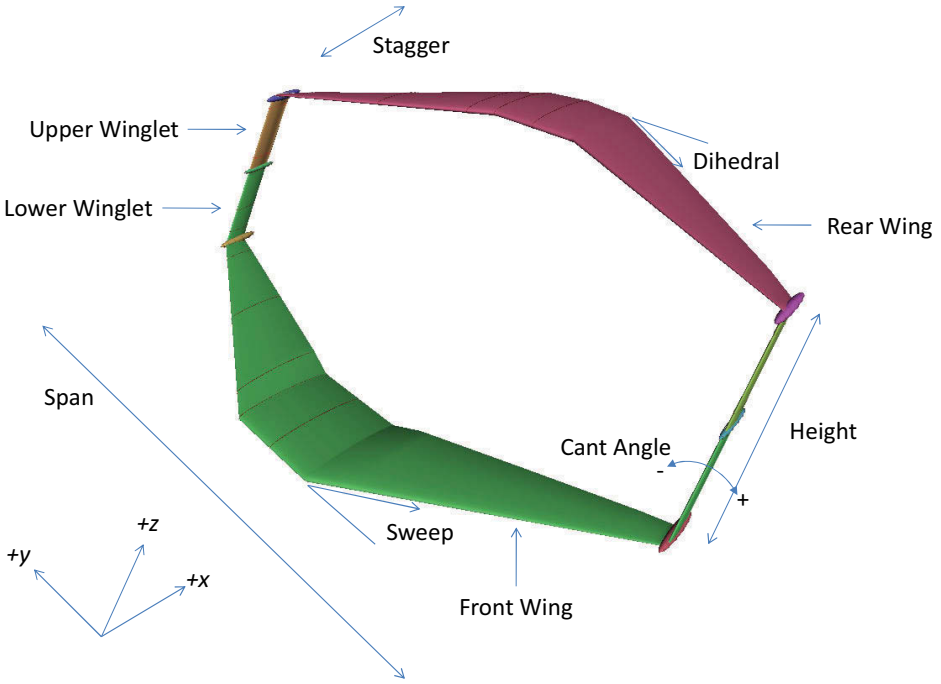

FIG 3. Box-wing geometry outlining main design variable

5. ANALYSIS WITH VORTEX LATTICE METHODS

Vortex lattice methods (VLM) are much like finite-element methods in which the aircraft surface is represented by different planforms. Each planform is subdivided into a finite number of elemental panels, on which classical equations and theorems are applied for computation of the aerodynamic forces. These panels are extended over the entire aircraft lifting surface both in spanwise and chordwise directions. Such methods are used in conceptual aircraft design studies and in aerodynamic investigations in general and have proven to be reasonably accurate and time efficient [11].

Main assumptions made in VLM analysis are steady, irrotational, inviscid, incompressible and attached flow. For preliminary design work, the Prandtl-Glauert correction is normally used to evaluate forces in compressible flows (Mach > 0.3).

5.1. Analysis with Tornado VLM

Tornado is a vortex lattice method programmed by Tomas Melin as part of his master thesis at KTH Stockholm. Over the time the code has matured and has been steadily updated and enhanced. It has also been compared with similar VLM and panel methods and has been found reliable. The code is provided under the GNU-General Public License and can thus be altered and modified without the permission of the author [11].

Tornado is based on MATLAB® environment and thus it is easily modifiable. The code supports any number of lifting surfaces arranged in any arbitrary fashion. Main outputs include lift, span loading, coefficient of lift (C_l) distribution along span, stability derivatives and induced drag prediction.

As mentioned earlier, the span loading for a box-wing design is very important and has to be a combination of a constant and an elliptical loading on main wings for obtaining minimum induced drag. To first comply with this basic requirement, Tornado's output was investigated. It was found that Tornado assumes the first defined surface to be as the main wing. Resultantly it only plots the span loading and C_l distribution for the first main wing. The code was altered and a plot of span loading for the second surface (2^{nd} wing) was included along with a reference plot of elliptical lift distribution. Further some changes in the code were made to lock the reference values to non-dimensional induced drag coefficient of multiple wing configurations.

Preliminary investigations were carried out to see the feasibility of the Tornado code for nonplanar geometries. Analyses were started by first analyzing known configurations. Three configurations of nonplanar design were modeled. These included wing with a winglet, biplane and box-wing design. All three were designed according to a height to span ratio of 0.2 so that there results can be compared with existing values in literature. Tornado's results were found to closely resemble the expected values from [2] and [12] as shown in Table 1.

As results from Tornado were found satisfactory further analysis on the biplane geometry was carried out. The biplane was chosen because at that moment the Tornado code was only plotting lift distributions for two main wings and plots of lift

distribution for winglets were not implemented yet. As the biplane wings were staggered, it was found that the span efficiencies decreased significantly and induced drag increased. Plots for staggered configuration were created and showed that both wings have different loading on them. To rectify this problem, wings have to be twisted to obtain again a similar and an elliptical lift distribution. At this point, several attempts were made by twisting individual wings but the right combination was not found as twisting one wing influences the second wing in a different way and this iterative procedure was not bearing any good results. Secondly, the final analysis was supposed to have a design variable of sweep for main wings. When wings are swept the angle of attack changes along the span and finding the right twist for analysis was seen as a major problem.

TAB 1. Span efficiency computed with Tornado and compared with [2] and [12] for height to span ratio of 0.2

Test Case	Span Efficiency Values		
	Kroo	Grasmeyer - IDRAG	Tornado
Wing-Winglet	1.41	1.453	1.1423
Biplane	1.36	1.358	1.3992
Box-wing	1.46	1.484	1.4781

At this moment it was decided to use a more suitable VLM code which can more efficiently capture nonplanar designs. This brief study showed that the results differ a lot when the basic requirement (appropriate span load distribution) behind the nonplanar concept is not fulfilled. This can result in wrong analysis and the researcher can be misled.

5.2. Analysis with IDRAG VLM

IDRAG is a code written by Joel Grasmeyer at Virginia Polytechnic Institute and State University. This program is specially created to calculate the induced drag of nonplanar lifting surfaces. It has both design and analysis capabilities. This means that either the spanload required to obtain the minimum induced drag can be found. Or if a spanload is included in the input, it finds the induced drag for the given set of surfaces. The program also calculates the span efficiency factor *e* [12].

Comparing with Tornado, IDRAG uses a different scheme for calculating induced drag. In IDRAG, computation of all forces is done in the Trefftz plane, which is a plane defined in the wake of the aircraft at infinity such that it is perpendicular to the wake. By using the Trefftz plane, the induced drag calculations are independent of the *x-coordinate, which effectively reduces the 3-dimensional problem to a set of 2-dimensional equations* [12]. This technique is based on Munk's theorem and for detail explanation [10] is recommended.

A typical IDRAG input file contains different reference values along with information regarding the geometry of the surfaces to be analyzed. To fix these reference variables like design lift coefficient, operating Mach number and other reference values, a single-aisle, twin engine, 150 PAX aircraft was chosen as the baseline aircraft having a wing reference area of 122.4 m^2 and total gross weight of 73 tonnes. Some of the values were computed based on available data, for example coefficient of lift was computed by using maximum take-off weight and cruise conditions. The Design lift coefficient was computed to be 0.67 and kept constant for reference and box-wing aircraft analysis and comparison. Furthermore, main wings for the box-wing configuration have equal wing areas (half of reference wing area) and contribute equally to the design lift coefficient i.e. each wing is supposed to produce design lift coefficient of 0.67.

In addition to this, a convergence study was carried out. To get familiar with the code several runs were conducted for known configurations. For convergence study it was found that the minimum number of panels which gave reasonable accuracy were 30 panels for each main wing and 10 panels for winglets (combined).

5.2.1. Selecting Design Variables

If a box-wing configuration is studied carefully several design features are present which need to be investigated. The features which are studied in this work are:

- Height to span ratio between main wings
- Aspect ratio for individual main wings
- Taper ratio, dihedral or anhedral
- Sweep and stagger

Some of the possible design configurations can be constrained by seeing the basic requirements of box-wing design. As stated earlier, a box-wing should have an equal distribution of lift among the two main wings. This restricts the studies from looking into unequal main wings for minimum induced drag condition. Similarly, different aspect ratios for individual wings don't make sense as both wings are having identical wing area and should have a maximum possible aspect ratio to achieve minimum induced drag (with structural constraints).

Other aspects for example airfoil selection and polyhedral wing shapes can be investigated too. As far as the airfoil selection is concerned, for this preliminary analysis it is not studied as the IDRAG code doesn't take into account an airfoil selection. Similarly, the polyhedral feature is not directly studied but can be inferred from the study of

dihedral and anhedral cases.

To facilitate the iterative procedure of investigating each design variable, a MATLAB® based script (*IDRAG_in)* was created which generated the input file for every individual case. The IDRAG input file requires corner points for defining the geometry of different surfaces. Based on the main design variables, a global set of parameters similar to design variables were passed on to this script which in return automatically defined a geometry based on input values.

Results of each design variations are discussed in following subsections.

5.2.2. Validation of Munk's Theorem

Several computation runs of individual values of stagger and sweep were made using the *IDRAG_in.m* file running on the IDRAG code. Positive stagger was varied from zero to five multiples of mean aerodynamic chord (MAC). Similarly, negative stagger was varied from zero to negative five multiples of MAC. For sweep both wings were independently varied from -45° to +45° quarter chord angles.

In all of these variations span efficiency factor and induced drag remained constant. Thus it can be concluded that the IDRAG code is computing the geometries correctly and is finding the similar optimum span loading for every run. These results validate the Munk's stagger theorem: box-wing design is independent of sweep and stagger if the correct span loading is maintained.

This has important consequences: If we can achieve similar drag reduction independent of sweep, transonic wings can be designed for a box-wing configuration. Wing sweep is an important factor by which the compressibility drag can be reduced during transonic speeds. It also allows for the use of higher thickness to chord ratio airfoils which result in lighter structure [13].

Stagger has similar advantages: by introducing stagger the interference of supersonic flow among the two main wings can be reduced at transonic speed. At the same time, increased stagger can positively influence the stability of the box-wing design. In other words, if the two main wings are in staggered position, the horizontal tail can be omitted from the design which further reduces the overall weight and the friction drag.

5.2.3. Height to Span & Aspect Ratio Variation

Height to span ratio variation along with aspect ratio was found to be the most important design variable for a box-wing aircraft.

Here the general trend for aspect ratio can be understood as that when a single wing is divided into two wings having the same total area and span as the original wing, maximum induced drag reduction is achieved [14]. In other words aspect ratio has been doubled for each individual wing and as per basic aerodynamics an increase in aspect ratio reduces the induced drag.

It is important to understand the relationship of aspect ratio and induced drag reduction of box-wing aircraft. If the full advantage of a box-wing aircraft is to be taken than the span of the two main wings for box-wing aircraft should be the same as that of a reference monoplane. In such condition maximum induced drag reduction is possible. The reduction increases as the gap is increased because the mutual interference factor between the two main wings is decreasing.

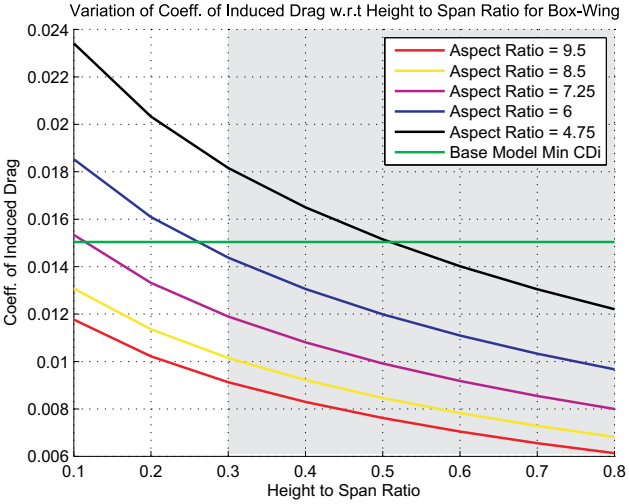

FIG 4. Variation of induced drag with height to span ratio

In this analysis, the aspect ratio for box-wing is calculated by considering the overall span of the configuration, shown in Figure 5. The reference area is taken as the sum of areas of the two main wings of the box-wing design.

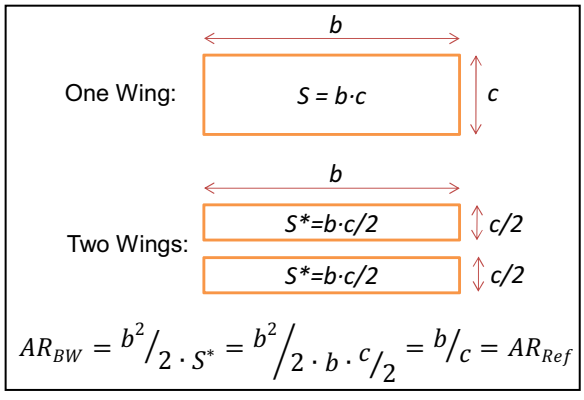

FIG 5. Definition of box-wing aspect ratio

If the aspect ratio (AR) of the reference aircraft is maintained for the individual wings of box-wing design (AR = 4.75 in Figure 4), then the box-wing aircraft will have even higher induced drag than the reference monoplane aircraft. Alternatively, if span is kept constant, a maximum reduction in induced drag

(AR = 9.5 in Figure 4) can be noticed. Figure 4 shows (green straight line) the minimum induced drag attained by the reference aircraft during its cruise phase (span efficiency factor of unity). With a decrease in aspect ratio the potential advantage of the box-wing aircraft subsides. For an intermediate aspect ratio this means, for example that a box-wing aircraft having an aspect ratio of 6.5 has to have a greater gap than a box-wing aircraft with an aspect ratio of 9.5 to significantly reduce the induced drag.

For a practical design, it is important here to take into account the effect of the lower chord value by choosing high aspect ratios as this will result in problems associated with low Reynolds number effects. Also structural design will get intensified as aspect ratio is increased.

5.2.4. Dihedral and Anhedral Variation

Furthermore, different dihedral angles for individual main wings have been investigated (Figure 6). The variation was conducted between 0° to 10° of dihedral for the lower wing and 0° to -10° of the anhedral for the upper wing. It can be seen that the maximum reduction is possible when choosing zero dihedral and anhedral angles for both wings.

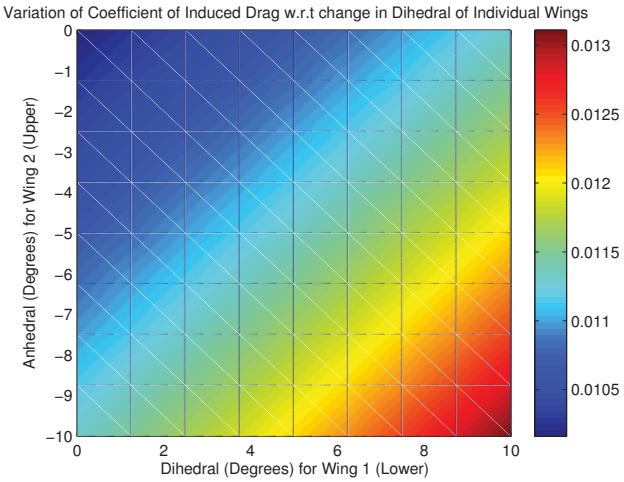

FIG 6. Variation of coefficient of induced drag with change in dihedral for individual wings

Once again it can be concluded that the general trend of effects of the dihedral angle are shown here, but the actual value being used in a box-wing design will also be dependent on structural and stability aspects of choosing the dihedral or anhedral angles.

5.2.5. Taper Ratio Variation

The taper ratio was independently varied for each main wing from 0.1 to 1, at an interval of 0.18. The 1 is representing an un-tapered wing. Several runs were made to assure that code was working fine. For every run it was concluded that for a box-wing, the taper ratio selection has no effect on its aerodynamic design. This can be explained as; the IDRAG code for every chosen taper ratio value readjusts the span loading so that the induced drag is minimized. Or in other words, any taper ratio can be chosen as long as the twist of the wing takes account of the required span loading.

Again the taper ratio selection is a function of aerodynamics as well as structures. This solution was run with an inviscid solver and thus doesn't take into account the low Reynolds number effect on wing tips if the wing is highly tapered.

5.2.6. Cant Angle Variation

Cant angle is defined as the mounting angle of the winglet with respect to the main wing. If the winglet is mounted perpendicular to the wing the cant angle is 0°. It is negative when the winglet is tilted towards the wing (inside) and positive for tilt direction away from the wing. When positive, it is increasing the effective span of a box-wing system. Thus it is expected to produce an induced drag reduction as effective span is increasing.

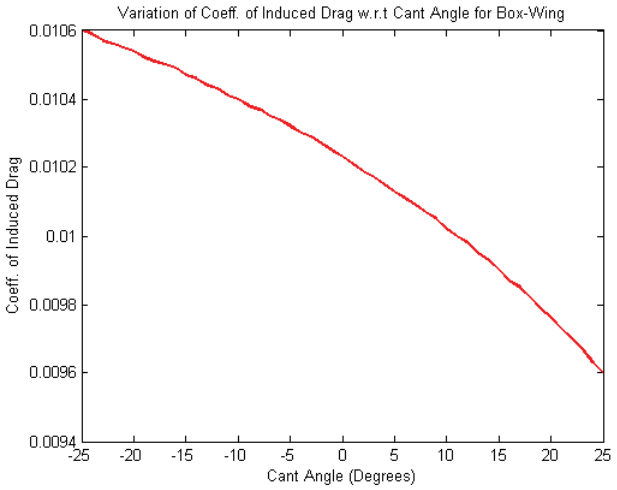

FIG 7. Variation of coefficient of induced drag with winglet cant angle

Figure 7, shows the variation of cant angle for a box-wing configuration. This cant variation was computed for a specific aspect ratio design but the variation is the same for any chosen span or aspect ratio. The desired aspect ratio (close to 9.5) for a box-wing design would probably not result in a good structural design. Thus, by choosing a lower aspect ratio a good design option can be achieved by positive cant angle winglets.

When studying the variation of before mentioned design parameters individually there is a chance that the global maximum of the design is not attained. With individual parameter sweeps, local maxima can be located for every variable but this can't guarantee that these local maxima would also lead to a global maximum, when all of the variables are considered collectively. To accomplish this task an algorithm was developed based on principles of genetic evolutionary processes [15] and [16].

5.3. Canonical Genetic Algorithm (CGA)

The operation of this algorithm starts off with the initialization of all design variables. Afterwards from the pool of design variables, random values are selected to form ten parents. This selection is random and every value of any variable has equal chance of being selected for formation of any of the parents. However, the values of design variables which are selected for one parent are not selected again for any other parent so that a more versatile group of parents can be formed.

After generation of ten parents, the program enters the optimization loop as shown in Figure 8. Than IDRAG is called through the intermediate script *IDRAG_in* mentioned before. Span efficiencies are evaluated and fed back to the optimization loop of the main code for every parent. Depending on span efficiencies parents are sorted out. Than the *best* five parents are saved separately while the lower five are sent to a crossover procedure.

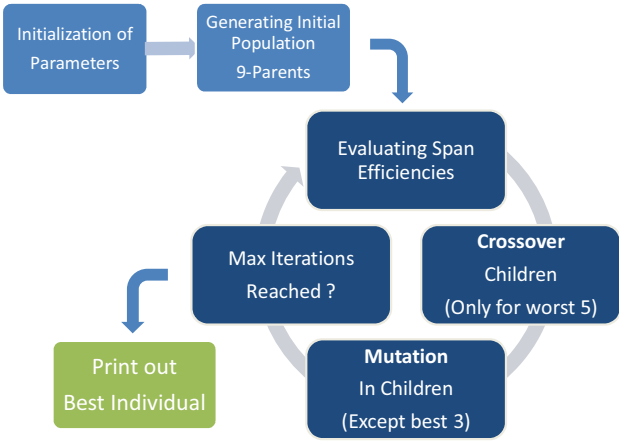

FIG 8. Canonical genetic algorithm flow chart

Crossover is an important random operator in CGA and the function of crossover is to generate a new "child" from the selected "good" parents. All five good parents are used in this process to create new five sets of *children* for further evaluation. All of the *bad* five parents are now replaced by these newly formed *children.*

At this point in the script, all of the values of variables being used in parents and new children are from the initial set of five good parents out of original ten parents. As the selection after initialization was made on random basis, it is less likely that the best combination of variables is among the first ten parents. Therefore after crossover, mutation is carried out. Mutation operates independently on the two old parents and new five children. The three best parents are left out of this process so that during an optimization the good qualities of the best three parents are not lost due to a random mutation. Mutation acts randomly on these seven parents, and introduces fresh values of design variables into their data sets. Later on during optimization if any of the parents gets a high span efficiency value it is moved to the best three accordingly thus gradually solving for the best combination.

After the mutation is complete all of these parents are again sent to the *IDRAG_in* file through a loop and the complete process is repeated. This cycle continuous till a convergence is met or the allotted loop limit is expired. After that the design variables for the evaluated best case are printed along with convergence plots.

The results of this study using CGA, concludes that the global minimum of induced drag for all design variables is located at local induced drag minimums of each design variable. As for a purely aerodynamic analysis this result was expected but if this optimizer is coupled with a structural design evaluator (having weight constraints) a more realistic final global maximum could be found using this code.

5.4. Selecting Configuration for CFD Analysis

For further exploring the box-wing design aspects and verifying the VLM results, a brief CFD study was carried out.

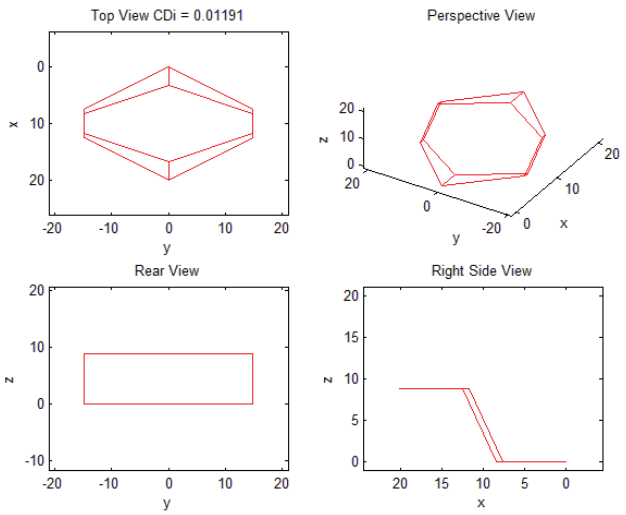

FIG 9. Selected box-wing configuration for CFD study

Selection of parameters was based on the results of CGA and parameter variations. The chosen aspect ratio is 7.25 for individual main wings with height to span ratio of 0.3 as shown in Figure 9.

Here it should be noted that the chosen box-wing configuration has overall lesser span than the reference aircraft while the reference area is kept constant (reference aircraft span: 34.1 m – selected box-wing span: 29.78 m). For the individual wings of the selected box-wing configuration more structural weight would be required due to higher aspect ratios. Additionally, the forward swept wing will have even higher weight due to extra stiffness requirements. However because of the presence of winglets joining both main wings at the tips a

positive structural influence can be obtained for the complete box-wing design.

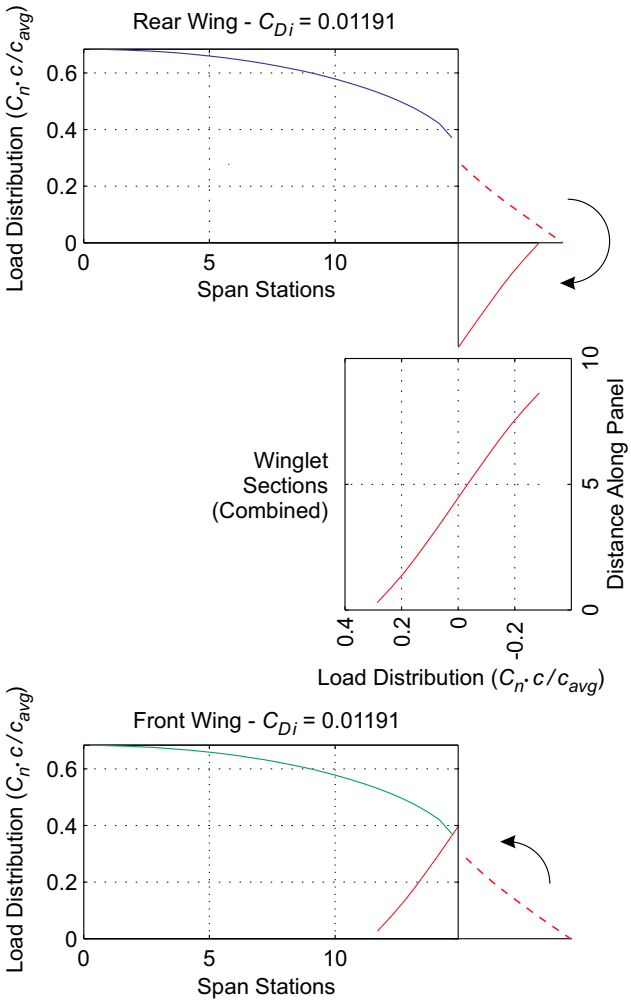

FIG 10. Computed optimum span load distribution for selected box-wing aircraft for CFD study

It can be assumed for analysis intent that the total weight of both configurations will remain the same. In doing so the design lift coefficient is kept constant during the cruise stage. The predicted coefficient of induced drag for these parameters is 0.01191 as compared to 0.01467 for the reference aircraft. This leads to an almost 20% reduction in induced drag. Here it should be noted that current civil transport aircraft are not designed to operate at their optimum span loading values. Under influence of structural weight constraints the span loading is restricted to more of a triangular distribution rather than elliptical. As for elliptical load distribution, the lift centre is located at 42.4 % of span (outward as compared to triangular distribution) thus resulting in heavier wings. So the induced drag value selected here for the reference aircraft is actually less as compared to practical design. Thus, in reality this can result in even higher drag reduction if the box-wing design is, instead of the reference aircraft, following an elliptical load distribution.

For this initial analysis no dihedral was taken into account and quarter chord sweep angle for main wings and winglets was chosen to be 25° which is the same as for the reference aircraft. Computed span loadings for the above configuration for minimum induced drag are shown in Figure 10. It can be seen that front and rear wing have identical, combined elliptical and a constant lift distribution. Prandtl suggested only elliptical loading but in a more exact solution, Frediani suggested an elliptical distribution added to a constant distribution [17]. The addition of constant distribution can be explained because of the presence of winglets. For optimally loaded wing-winglet combination such distributions are formed. For winglet sections, the optimum distribution is almost triangular as shown in Figure 10.

5.5. Calculating Geometric Twist by LAMDES VLM

LAMDES was used to calculate the twist required to maintain the span loading calculated by IDRAG in the previous step.

LAMDES is a VLM optimization code and was written at Virginia Polytechnic Institute and State University. This code can also handle nonplanar surfaces but is limited to only two surfaces. It can find the surface twist needed to attain the minimum induced and pressure drag coefficients [4].

Initially, it was intended to model a complete box-wing in LAMDES such that the estimates from IDRAG can be re-confirmed. Due to the limitation of the code, the box-wing was to be modeled as two wing-winglet combinations. During the test runs, it came out that LAMDES is not able to compute geometric twist angles for the winglet surface completely. The twist distribution along span is only computed for the main wing and the winglet is left out. As for the box-wing configuration, winglets carry their own specific loadings. Thus it was decided to model each surface individually.

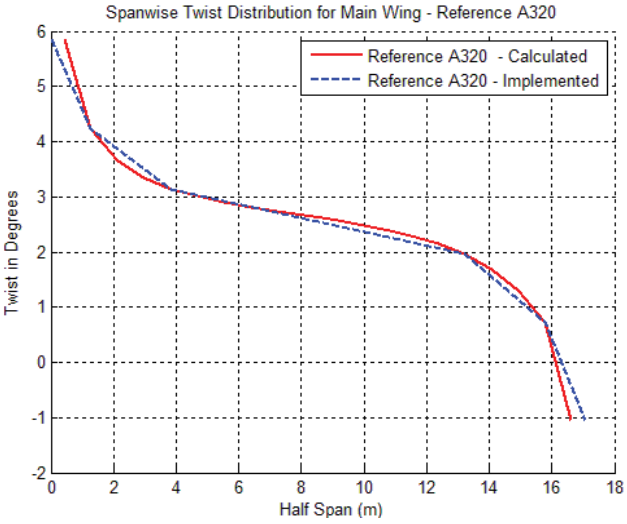

FIG 11. Spanwise twist distribution for reference wing calculated

Another limitation of the code was found to be that the code assumes a chordwise loading for NACA 6 series airfoil sections. Nevertheless, the code can be used for initial estimates on twist distribution for the transonic regime too [18].

The reference wing, a single surface configuration, was modeled completely in LAMDES. Figure 11 shows the twist distribution along the span. Having a swept aft wing, the twist distribution is following the theoretical trend and has been computed for elliptical span loading. The characteristic of the curve is changing at 5 m span station due to change in chord length where the engine pylon is attached along with the main landing gear assembly. This change was expected as for a sudden variation in chord along the span. The twist rises up to compensate the loss of lift. The sudden spanwise change in chord distorts the 3-D flow and thus causes a loss of lift. The dotted blue lines show the implemented twist of the later model of the reference wing.

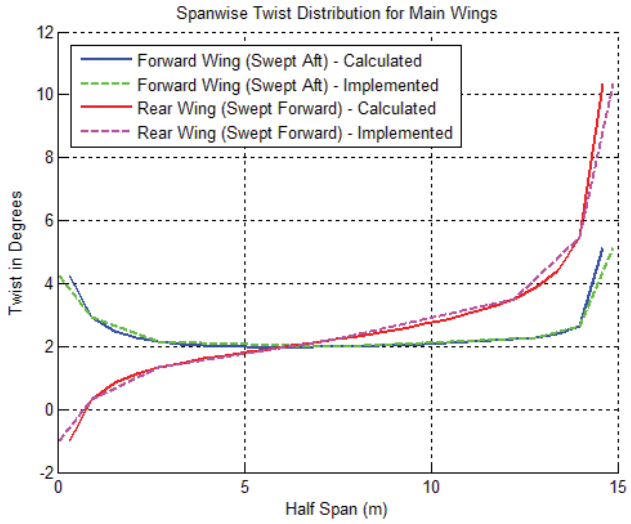

FIG 12. Spanwise twist distribution for main wings of selected box-wing configuration

For box-wing calculations, the IDRAG span loading was imported into the LAMDES file and each surface was dealt individually. LAMDES was bound to estimate the geometric twist on given span loading. Figure 12 shows the twist calculated for individual main wings of the selected box-wing configuration. It can be seen that the twist distribution trend for a swept aft and swept forward surface is in accordance with the theory. The wings are heavily loaded towards the tip. Thus, for a swept aft wing the twist distribution rises up again near its tip region. Similarly, for a swept forward wing from basic aerodynamics the effective angle of attack increases along the span from tip to root. To maintain the high loading the tip is at high angle of attack and the root even goes down to negative. Here it should be kept in mind that the local chord distribution along the span is also affecting the amount of twist needed at a particular span station.

Several span stations were selected along the span, to construct the 3-D model of the box-wing for further analysis. For both wings, 6 span stations are being used to fully capture the twist along the span; this implemented twist is shown by the dotted lines above.

Similarly, each winglet section was modeled separately in LAMDES. The lower winglet was modeled from root to tip and the upper winglet was modeled the other way around i.e. from tip to root. This resulted in similar curves as of Figure 12 (plots not shown due to similarity of results).

6. ANALYSIS WITH EULER CFD METHOD

The Euler method or the Euler equations by definition neglects the viscous component of the 3-D flow field. The flow is assumed to be unsteady and rotational in nature, but still capable of describing shock waves (compressibility effects) and fairly good in predicting lift. The drag prediction by choosing the Euler methods is limited to induced drag and compressibility drag. For this preliminary analysis, the Edge solver was used, which is a CFD flow solver for unstructured grids developed by the Swedish Defense Research Agency (FOI).

To conduct an Euler solution for the selected box-wing configuration, a detailed geometrical model was required. This task was accomplished by using SUMO, a rapid aircraft geometry modeler. SUMO is provided by Larosterna Engineering Dynamics. It is being developed as part of the EU funded SimSAC project [19].

In SUMO, individual sections of aircraft can be designed on a modular basis, where the fuselage can be defined from its top and side view cross-sections and the wing can be modeled by defining airfoil sections at different spanwise locations. This rapid modeling capability of the software helped a lot during the current study. Several airfoil and wing incidence changes were implemented quickly and effectively. SUMO also generates automatically an unstructured triangular surface mesh of the defined model.

A volume mesh around the surface mesh can also be created using the TetGen, developed by the Numerical Mathematics and Scientific Computing research group at Weierstrass Institute for Applied Analysis and Stochastics, Berlin [20]. By defining appropriate 3D volume mesh parameters a volume mesh can be created based on the surface mesh in SUMO.

Using the rapid modeling techniques in SUMO, a reference wing and a box-wing were created. Only wing sections were modeled as analyzing a complete aircraft was not considered suitable at this primary analysis phase. For transonic wings the airfoil selection is dependent on cruise speed, wing sweep and design lift coefficient. All these

parameters are known from reference aircraft data. In addition to this, thickness to chord ratio for this analysis was calculated using cruise Mach number and wing quarter chord sweep [21]. Thickness to chord ratio obtained from [21] amounts to 0.11. Using this thickness to chord ratio and the design lift coefficient, NASA SC(2)-0612 airfoil was selected as possible airfoil for both designs.

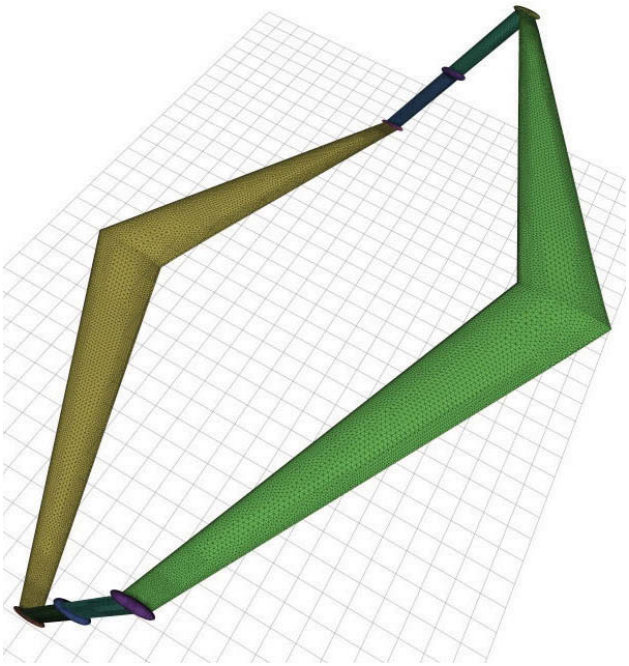

FIG 13. Surface mesh created in SUMO for selected box-wing configuration

Afterwards reference wing and box-wing were modeled in SUMO. Choosing appropriate chord stations along span, the LAMDES calculated twist was implemented with the restriction that between each chord stations the variation of twist was linear. The final geometrical model of a box-wing having a surface mesh is shown in Figure 13. The surface mesh created for this study had a mesh density of around 0.2 million triangles. The final volume mesh had a density of 1.7 million quadrilaterals. Considering the primary nature of the analysis, a 1.7 million mesh density was found suitable in comparison with other studies of similar nature using inviscid solvers [18].

For inviscid drag comparison, the design lift coefficient is equalized between different geometries. Using the LAMDES twist it was found that the reference design lift coefficient of 0.67 was being achieved around 0° angle of attack. Thus, twist estimations were correct to some extent.

For low subsonic (Ma = 0.3) the proposed reduction in induced drag was captured as shown in Table 2. The difference in VLM and CFD results might be due to an approximation of the geometrical model and differences in selected airfoils for LAMDES calculations and CFD analysis.

The rise in drag coefficient at a transonic Mach number of 0.78 is due to the presence of strong shock waves over the wing surfaces thus causing an additional compressibility drag along with induced drag. These shocks can be seen in Figures 14 and 15, which are depicting the Mach contours of the analyzed geometries.

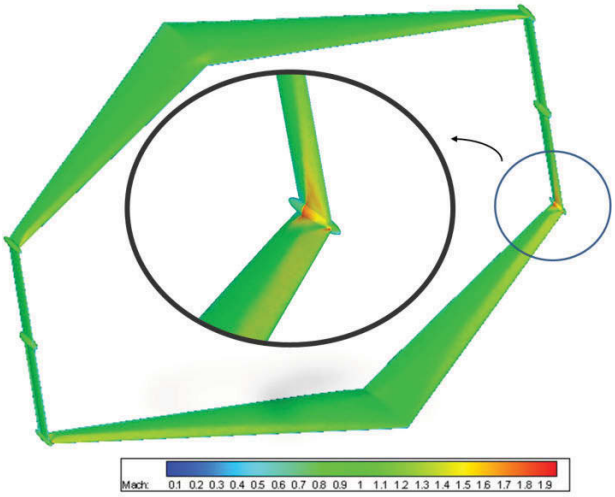

FIG 14. Mach contours for selected box-wing configuration wing at cruise conditions

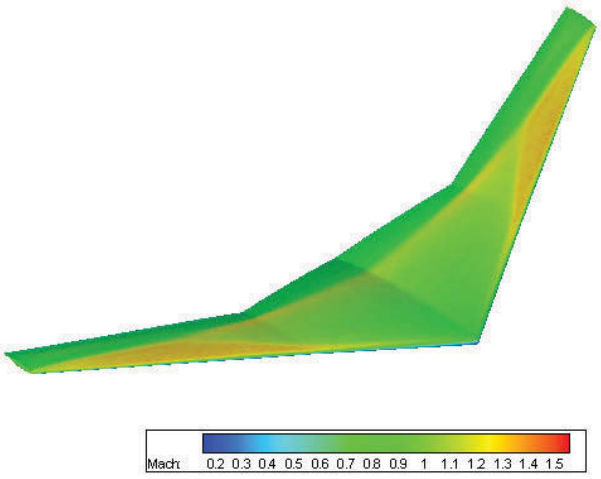

FIG 15. Mach contours for reference wing at cruise conditions

To obtain a low induced drag from a box-wing configuration it is essential that both winglets produce a specific side force as shown previously in Figure 2. For the lower winglet, this side force is generated inwards while for the upper one, it is the other way around. As part of VLM analysis, this specific lift distribution was calculated and is shown in Figure 10. It is important to highlight that, because of the presence of winglets, both main wings do not go to zero span loading at their tips. Instead they retain a constant value. To achieve this span loading, VLM analysis calculated high values of geometric twist for tip regions as shown in Figure 12.

TAB 2. Comparison of Euler CFD results at different Mach numbers for height to span ratio of 0.3

	$C_{Di,Ref}$ [cts]	$C_{Di,BW}$ [cts]	e_{Ref} [-]	e_{BW} [-]	E_{Ref} [-]	E_{BW} [-]	$E_{max,Ref}$ [-]	$E_{max,BW}$ [-]	ΔE_{max} [%]
VLM	147	119	1.036	1.654	21.50	23.58	21.53	23.90	11.0
Euler (*Ma* = 0.30)	198	175	0.768	1.266	18.46	19.71	18.53	19.72	6.4
Euler (*Ma* = 0.78)	199	280	0.543	0.703	×	×	×	×	×

With an estimated $E_{max,Ref,init}$ = 19.45 for initiating calculations with $C_{D,0}$ to obtain values of E_{max}

Consequently, the main wing tips are heavily loaded and this results in the potential increase of compressibility drag for box-wing design (Figure 14). It can also be seen in the analysis that the Mach number is considerably higher in tip regions due to the excessive incidence implemented in these regions.

Several attempts were made to obtain results for grid convergence studies. However, problems were encountered during surface mesh generation and refinement. Results obtained from the Euler method are of preliminary nature and more effort should be spent on refining the model and grid. Additionally airfoil selection can be revised to further investigate the increase in compressibility drag. That is, the induced drag reduction for box-wing is shown compared to conventional designs. Secondly, suitable airfoil selection came out to be an important issue in successful box-wing design. The supersonic flow over the box-wing configurations is not satisfactory and thus in future, airfoil selection can be added as major design issue for box-wing configuration.

The box-wing configuration selected for this CFD analysis is based on the assumption that total lift coefficient and wing area remain the same for reference and box-wing design (Equation 3).

(3) $$mg = \frac{1}{2} \cdot \rho \cdot V^2 \cdot C_L \cdot S_{Ref}$$

Furthermore for the chosen box-wing configuration, the aspect ratio was reduced from 9.5 to 7.25 while the span efficiency was increased from 1 to 1.654. This means, the resultant reduction in induced drag is achieved even at a lower value of aspect ratio (Equation 2).

Maximum lift to drag ratio is a key variable in expressing the aerodynamic efficiency of a design. To gather L/D_{max} out of calculated C_{Di}'s and e's, $C_{D,0}$ had to be estimated from Equation 5:

(4) $$E_{max,Ref,init} = 19.45$$

(5) $$C_{D0,ref} = \frac{\pi \cdot AR \cdot e}{4 \cdot E_{max,Ref,init}}$$

At this stage of preliminary analysis, it is assumed that the wetted area of the box-wing aircraft is equivalent to the wetted area of the reference aircraft:

(6) $$\left(\frac{S_{WET}}{S_W}\right)_{ref} \approx \left(\frac{S_{WET}}{S_W}\right)_{BW}$$

The same applies to the equivalent skin-friction coefficient. Thus:

(7) $$C_{D0} = C_{fe}\frac{S_{WET}}{S_W} \Longrightarrow C_{D0,ref} \approx C_{D0,BW}$$

The lift coefficient for minimum drag can be calculated from:

(8) $$C_{L,md} = \sqrt{C_{D0} \cdot \pi \cdot AR \cdot e}$$

As aircraft mass and wing have been kept constant, C_L was kept constant as well. Thus, C_L / $C_{L,md}$ can be calculated. The drag coefficient can be calculated using Equation 1.

Using above relation, actual C_L over C_D ratio can be obtained. E_{max} can be derived from Equation 9:

(9) $$E_{max} = \frac{E}{\frac{2}{\frac{1}{\left(\frac{C_L}{C_{L,md}}\right)} + \left(\frac{C_L}{C_{L,md}}\right)}}$$

This approach has been applied to reference wing and box-wing values. Results are depicted in Table 2 and show that the significance of the box-wing potential is lower than actually thought of before.

Theoretically, a further increase in E_{max} could be achieved by setting the *AR* of the box-wing equal to that of the reference wing. This can be seen in the following context:

(10) $$E_{max} = \frac{1}{2}\sqrt{\frac{\pi \cdot e \cdot AR}{C_{D0}}}$$

(11) $$\frac{E_{max,BW}}{E_{max,ref}} = \sqrt{\frac{AR_{BW} \cdot e_{BW}}{AR_{ref} \cdot e_{ref}}}$$

Thus, the following conclusion can be drawn: To exploit the full potential of a box-wing design, the *AR* should be kept as close as possible to the reference

AR and *e* must be increased as much as possible (which results into a higher $C_{L,md}$) by e.g. increasing the height to span ratio. However, both considerations are limited by structural reasons and low Reynolds number effects.

The box-wing design that has been chosen for analyses exhibits therefore a further potential in increasing E_{max}. This is because the box-wing has a high span efficiency which allows it to be operated at higher C_L values during cruise. If C_L is increased according to Equation 3, than a lesser wing area would be required for the complete box-wing design as it would be operating at a higher design lift coefficient. This constellation is more favorable in terms of maximizing *E*.

With *e* values found in literature (Table 1) an increase in 31.9 % of E_{max} would become possible if the *AR* is kept constant.

7. BOX-WING CONFIGURATION AS A POTENTIAL CIVIL TANSPORT AIRCRAFT

Nowadays aircraft performance is not restricted to just improvements in cruise performance or short take-off and landing capabilities. With a growing number of air traffic, space congestion, both on and off ground, is becoming more vital than ever before. The success of a novel concept in future truly lies in all aspects of civil aircraft operations. At the current stage it would be almost economically impossible for the aviation industry or the airport operators to adopt a completely new design having all-together different operational requirements. Similarly, as this study was carried out in the context of the *Airport 2030* project it was important to cover the aspects of box-wing design in the light of common airport issues [23].

Secondly, from the work done in previous section it can be concluded easily that there exists a potential decrease of induced drag for a box-wing configuration. By applying a more general approach it was decided to outline all the aspects of box-wing aircraft operations and not just the in-flight performance improvements for different categories of civil transport aircraft. Thus, in the following sections, the potential advantages of box-wing design (both in air and on ground) as a single aisle aircraft, long endurance aircraft and as a very large aircraft concept are outlined.

7.1. Box-Wing Potential as a Single Aisle Aircraft

This market is rapidly growing with the introduction of low-fare airlines. The two main aircraft in this category are the Boeing 737 and the Airbus A320 (shown in Figure 16 is a single aisle box-wing concept).

The key points in this study are summarized as:

- Performance improvement in cruise stage
- More efficient during successive take-offs and landings
- Commonality with existing aircrafts – same fuselage section
- Ease in airport congestion as it requires less parking and handling space
- Similar STOL design can be incorporated

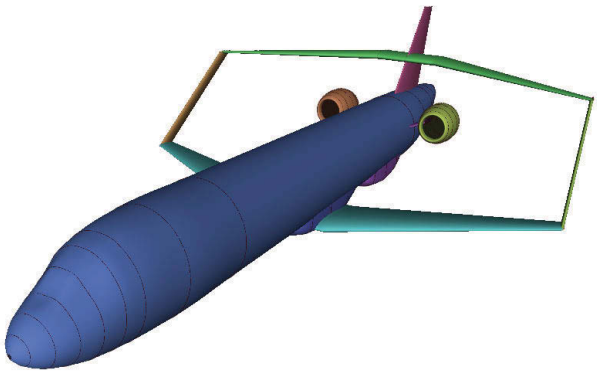

FIG 16. Box-Wing version of single aisle aircraft

7.2. Box-Wing Potential as a Long Endurance Aircraft

To achieve high endurance for such aircraft, an extra long span would be required. High aspect ratio wings are serving best for this purpose. As noted earlier in the background section, high aspect ratio wings have two main problems. Firstly, with increase in span the wing weight increases. Secondly, practical problems occur during ground operations for aircraft with very high span. A box-wing long endurance aircraft can possibly eliminate both of the problems. According to recent research in the field, a box-wing aircraft might even prove to be structurally stiffer than conventional designs thus allowing higher aspect ratios for individual wings of the box-wing design [22].

7.3. Box-Wing Potential as a Very Large Aircraft

As the volume of air passengers grow rapidly the aviation industry has keen interest in this category of civil aircrafts. For upcoming VLA designs, airport operations and compatibility plays an important role.

The potential advantages in this category can be summarized as:

- Performance improvement during cruise, takeoff, climb and landing can be expected at similar or even smaller total wing span.
- Box-wing favors double deck design as it helps to improve height to span ratio for the complete design.
- Ease in terminal restrictions and maneuver envelope at airports.
- Similar emergency requirements due to commonality in fuselage design (in comparison to blended wing body design).

- Ease in wake-vortex requirements.

The reduction in noise and emissions are major goals for future air travel. By choosing novel concepts like box-wing with improved power plant technologies new possibilities emerge to reduce both emissions and noise. Lesser drag means lesser power requirements, thus lesser impact on the environment through emissions. Similarly, noise can be reduced by shielding the engines in the aft fuselage section between the twin vertical fins. Several other engine installation options are available in a box-wing if further explored.

8. CONCLUSIONS AND RECOMMENDATIONS

Following conclusions can be drawn for nonplanar systems from this study:

- Nonplanar systems show capabilities to reduce the induced drag significantly.
- The reduction is mainly due to overall reduction in the downwash of the complete system.
- Increase in aspect ratio by dividing a surface into two or more similar span surfaces having same total wing area can considerably reduce the induced drag.
- Similarly, adding a winglet or an endplate to a lifting system further reduces the downwash and increases the overall span efficiency of the system.

For the analysis of nonplanar systems it can be concluded that vortex lattice codes can be utilized. Here two important conclusions can be drawn from this work:

- An appropriate span loading should be established and maintained throughout the analysis of a nonplanar system.
- Care must be taken while defining span efficiency and aspect ratio of the individual lifting surfaces and as a whole for the complete lifting system.

As far as the box-wing design variables are concerned, it can be concluded:

- Stagger, sweep and taper ratio has no effect on the complete induced drag of the system if adequate span loading is maintained.
- Induced drag increases with an introduction of a dihedral into the system.
- Height to span ratio is the most important variable which directly influences the overall efficiency.
- Further improvement can be made by adjusting the cant angles of the winglets.

For CFD analysis it can be concluded:

- Transonic airfoil selection is identified as one of the important design variables.

During operation, a box-wing as a very large aircraft seems to be the most appropriate application, as it can prove to be a good solution for ground operational problems and at the same time minimizing low Reynolds number effects in the box-wing VLA case.

Furthermore, viscous effects were neglected in this analysis. These effects should however be investigated and taken into consideration for a more detailed analysis. A coupled analysis of aerodynamics, structures and stability calculations should be conducted. However, at this stage none of the known aircraft design programs are written to capture the closed wing system of a box-wing design. Much effort is necessary to adapt such programs.

ACKNOWLEDMENT

This work was completed as part of a student Master Thesis. The author wants to acknowledge the support of staff at the Aircraft Design and Systems Group at HAW Hamburg. The author would also like to express his gratitude towards Erasmus Mundus Space Master program for financial support for his master studies. The financial support by the Federal Ministry of Education and Research (BMBF) and the support of the Hamburg State Ministry of Economic and Labor Affairs (BWA) are gratefully acknowledged [23].

NOMENCLATURE AND ABBREVIATIONS

AR	Aspect Ratio
b	Span [m]
C_D	Coefficient of Drag
C_L	Coefficient of Lift
$C_{L,md}$	Coefficient of Lift at Minimum Drag
C_{Dc}	Coefficient of Compressibility Drag
C_{Do}	Coefficient of Zero Lift Drag
C_{Di}	Coefficient of Induced Drag
CFD	Computational Fluid Dynamics
D	Drag [N]
E	Lift to Drag Ratio
E_{max}	Maximum Lift to Drag Ratio
e	Oswald's / Span Efficiency Factor
g	Acceleration due to Gravity [m/s^2]
h	Vertical Distance Between Main Wings of Box-Wing [m]
MAC	Mean Aerodynamic Chord [m]
m	Mass [kg]
ρ	Density [kg/m^3]
S	Wing Area [m^2]
V	Velocity [m/sec]
VLA	Very Large Aircraft
VLM	Vortex Lattice Method

REFERENCES

[1] BUSQUIN, P.; ARGUELLES, P.; BISCHOFF, M; et al.: European Aeronautics: a Vision for 2020. European Community, Brussels. 2001

[2] KROO, I.: Nonplanar Wing Concepts for Increased Aircraft Efficiency. VKI lecture series on Innovative Configurations and Advanced Concepts for Future Civil Aircraft. 2005

[3] FREDIANI, A.; RIZZO, E.; BOTTONI, C; et al.: The Prandtl Plane Aircraft Configuration. Aerodays, Vienna. 2006

[4] MASON, W. H.: Applied computational aerodynamics text/notes. 1995. Retrieved April 2010,from URL: http://www.aoe.vt.edu/~mason/Mason_f/CAtxtTop.html

[5] KROO, I.: Drag Due to Lift: Concepts for Prediction and Reduction. Annual Review Fluid Mechanics, Pg: 587-617. 2001

[6] COLLINS, T. D.: Analysis of A380 Transport. Department of Aerospace and Ocean Engineering, Virginia Polytechnic Institute and State University, 2001. Retrieved March 2010. URL:http://www.aoe.vt.edu/~mason/Mason_f/A380Collins.pdf

[7] PRANDTL, L.: Induced Drag of Multiplanes. NACA TN 182. 1924

[8] FREDIANI, A.; RIZZO, E.; BOTTONI, C; et al.: A 250 Passenger Prandtlplane Transport Aircraft Preliminary Design. XVII Congresso Nazionale AIDAA, Rome. 2005

[9] FREDIANI, A.; CREMA, L.B.; CHIOCCHIA, G; et al.: Development of An Innovative Configuration for Transport Aircraft; A Project of Five Italian Universities. XVII Congresso Nazionale AIDAA, (Pg: 2089 – 2104) Rome. 2003

[10] GALL, P. D.: An Experimental and Theoratical Analysis of the Aerodynamic Characteristics of a Biplane-Winglet Config. 1984. NACA TM 85815.

[11] TOMAS, M.: A Vortex Lattice MATLAB Implementation for Linear Aerodynamic Wing Applications. Department of Aeronautical and Vehicle Engineering, Royal Institute of Technology (KTH). 2000

[12] GRASMEYER, J.: A Discrete Vortex Method for Calculating the Minimum Induced Drag and Optimum Load Distribution for Aircraft Configurations with Noncoplanar Surfaces. Department of Aerospace and Ocean Engineering, Virginia Polytechnic Institute and State University. 1997

[13] OBERT, E.: Aerodynamic Design of Transport Aircraft. Delft University of Technology. Faculaty of Aerospace Engineering. Section Design of Aircraft and Rotorcraft. IOS Press, Netherland. 2009

[14] RAYMER, D. P.: Aircraft Design: A Conceptual Approach. American Institute of Aeronautics and Astronautics, Inc., Washington, DC. 1992

[15] HOLLAND, J.: Adaption In Natural and Artificial Systems. University of Michigan Press, Ann Arbor, 1975

[16] RUSSEL, J.R.; NORVIG, P.: Artificial Intelligence: A Modern Approach. Prentice Hall Series. 2nd Edition, 2003

[17] BUTTAZZO, G. (ed.); FREDIANI, A. (ed.); MONTANARI, G.: Best Wing System: An Exact Solution of the Prandtl's Problem. Variational Analysis and Aerospace Engineering - Springer Optimization and Its Applications, Volume 33, 1999

[18] ANDY, K.; MASON, W.H.; GROSSMAN, B; et al.: A-7 Strut Braced Wing Concept Transonic Wing Design. Department of Aerospace and Ocean Engineering, Virginia Polytechnic Institute and State University, 2002

[19] ELLER, D.: Aircraft Modeling and Mesh Generation, 2009. Retrieved March 2010, from Larosterna Engineering Dynamics, - URL: http://www.larosterna.com/sumo.html

[20] SI, H.: TetGen - A Quality Tetrahedral Mesh Generator and a 3D Delaunay Triangulator, 2009. Retrieved March 2010. URL: http://tetgen.berlios.de/

[21] SCHOLZ, D. (ed.): Aircraft Design. Hamburg University of Applied Sciences, Department of Automotive and Aeronautical Engineering, Aircraft Design and Systems Group (Aero), Short Course Notes, 2008. URL: http://flugzeugentwurf.de

[22] CRANFIELD UNIVERSITY: The Design of a Novel Box-Wing Medium Range Airliner: The A-9 Dragonfly, Retrieved March 2010. URL:http://www.cranfield.ac.uk/soe/departments/aerospaceengineering/page47131.html

[23] AIRPORT 2030: Airport 2030 Project, HAW Hamburg. URL: http://Airport2030.Profscholz.de/